A static test method to assess swivel seat strength in frontal impact

Preston, R., Amato, G., Lyons, M., & Simms, C. (2014). A static test method to assess swivel seat strength in frontal impact. *International Journal of Crashworthiness*, *19*(5), 469-483. https://doi.org/10.1080/13588265.2014.914667

Published in:
International Journal of Crashworthiness

Document Version:
Peer reviewed version

A Static test method to assess swivel seat strength in frontal impact

Ross Preston[1], Giuseppina Amato[2], Mathew Lyons[3], Ciaran Simms[4]

Abstract

Mechanical swivel seat adaptations are a key aftermarket disability modification to any small to medium sized passenger vehicle. However, the crashworthiness of these devices is currently unregulated and the existing 20 g dynamic sled testing approach is prohibitively expensive for prototype assessment purposes. In this paper, an alternative quasi-static test method for swivel seat assessment is presented, and two different approaches (free body diagram and multibody modelling) validated through published experimental data, are developed to determine the appropriate loading conditions to apply in the quasi-static testing.

Results show the two theoretical approaches can give similar results for estimating the quasi-static loading conditions, and this depends on the seatbelt configuration. Application of the approach to quasi-static testing of both conventional seats and those with integrated seat belts showed the approach to be successful and easy to apply. It is proposed that this method be used by swivel seat designers to assess new prototypes prior to final validation via the traditional 20 g sled test.

Keywords Swivel seat adaptations, quasi-static testing, integrated seat belts, MADYMO.

[1] McElmeel Mobility Group, 15 Ballyscandal Road Armagh, Co. Armagh, Northern Ireland BT61 8BL, UK, email: rossjpreston@gmail.com

[2] School of Planning, Architecture and Civil Engineering, Queen's University Belfast, Belfast, UK

[3] Mechanical Engineering Department, Trinity College Dublin, Dublin, Ireland, email: mathew.lyons@gmail.com

[4] Mechanical Engineering Department, Trinity College Dublin, Dublin, Ireland, email: csimms@tcd.ie

Introduction

Mechanical swivel seat adaptations are a key aftermarket disability modification to any small to medium sized passenger vehicle. They allow the vehicle's passenger or driver's seat to rotate 90 degrees out through the opened door. This eases access for individuals with limited mobility, especially with restricted lower body strength and movement. The nature of the adaptation and the size of the industry mean that businesses performing seat conversions are mostly Small to Medium sized Enterprises (SMEs) who source a generic swivel seat base from a main supplier and adapt each base to fit the specific vehicle model they are working with for a given client.

It is well established that the seating system of a vehicle is a key occupant protection device in the event of a collision[1]. In a frontal collision, the loads on the seat are high due to the mass of the occupant and the configuration of the seatbelt system and the seat must deform to facilitate energy absorption but retain integrity to prevent occupant ejection. Accordingly, new vehicles in Europe are legally obliged to adhere to regulations outlined by the United Nations Economic Commission for Europe (UNECE)[25].

UNECE Regulation 17 outlines the testing that must be performed on all seats and seat base designs before they can be fitted to vehicles. In the Unites States FMVSS 208 [26] gives similar requirements . However, a swivel seat conversion does not fall under any UNECE regulations, as the adaptation is carried out after the vehicle has been registered in its specific country. Some European countries also have their own individual requirements in addition to the UNECE regulations and in future the post registration adaptation of vehicles may become more regulated. However, at present, once a vehicle model has been registered, there are no official requirements for a vehicle adapter to adhere to.

Swivel seat bases are generally composed of two parallel plates separated by an off-centre bearing replacing the original seat anchor points and this system is inserted between the original vehicle seat and the vehicle floor, see Figure 1. The off-centre bearing between the two plates allows the seat to rotate from its original position to one facing out of the vehicle and protruding over the door sill. Existing products are similar designs that can be time consuming to fit, heavy duty and over-engineered, probably due to minimal testing at the product design stage. Since the integrity of the seat is crucial for occupant protection in a collision, vehicle adaptation companies need to ensure that the adaptation does not compromise the safety of the seat or weaken the surrounding structure of the vehicle. However, since there are no applicable standards, a level of self-regulation is required and there are no current guidelines to follow.

Our review found no literature directly relating to swivel seat strength requirements for automotive safety. Shaheen and Niemeier [21] discuss the requirement for vehicle adaptations to allow the increased mobility of older people. However, there is no direct analysis of swivel seat adaptations.

In contrast, there is a much broader range of literature relating to conventional seat design [2, 14, 28] and seat with integrated seatbelts [5-7, 19]. Early work with impact sleds and crash test dummies established a clear relationship between seat design and occupant injury risk[1]. This approach was extended with an instrumented crash test rig

and FE modelling to assess whiplash and submarining risk [9, 13].

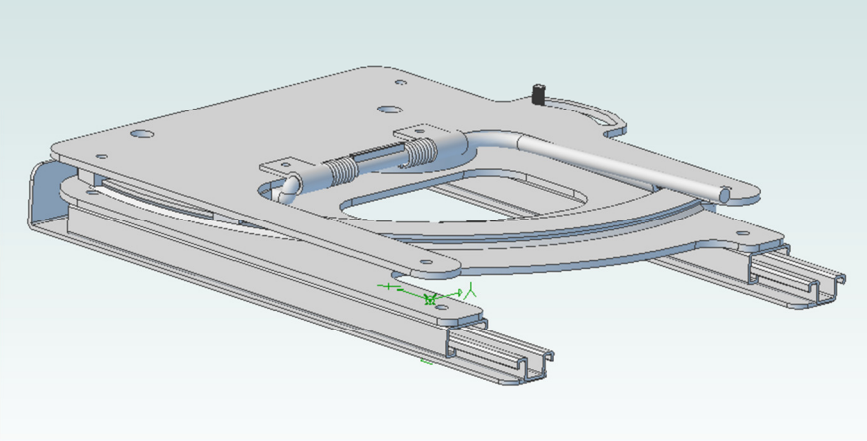

Figure 1 – Swivel seat design.

The use of multibody dummy models for assessing injury risk in vehicle crashes is well established in the literature [3, 10, 15, 16, 18], also coupled to FE analysis as in [4, 11]. MADYMO effectiveness in ascertaining the relationship between the vehicle component and the occupant response in frontal and rear impacts is also established in a number of studies, among these:[8]for the front and rear seats, [17, 29] for seat belt configurations, [20] for counter balanced motion seat, [15, 27] for high back booster seats.

The design and analysis of a powered swivel seat, including dynamic finite element analysis to assess the impact response is presented in [22]. However, this approach requires significant computational modelling skills and is unlikely to be practical for an SME in evaluating a potential swivel seat design.

The purpose of this paper is therefore to outline a quasi-static cost-effective testing procedure for swivel base designs. The procedure is derived from the loading criteria outlined in the UNECE Regulation 17. The aim of the proposed alternative test is to ensure that swivel bases can withstand the required loads in the case of a representative frontal collision to ensure occupant retention. Moreover, the objective is to present a method which allows producers of swivel bases to perform a preliminary test of their product within a more acceptable budget than would be required for full scale dynamic testing.

The methods used to derive the peak loading estimates for the quasi-static testing are both the generic free-body diagram approach and multibody modelling. The first yields a linear system of 7x7 equations with input parameters which can be adapted to specific seat geometries and that can be readily solved using a spreadsheet. Therefore the need for expensive dynamic testing and detailed computational modelling is removed.

The static test procedures proposed are applied to test the adaptations of two new swivel base designs to two commercial seats: The first swivel model is intended to fit a standard vehicle seat; the second design is intended for vehicle models where seatbelts are integrated into the seat and which results in much greater loading of the swivel base in the event of a frontal collision.

Methods

The dynamic test procedure defined in UNECE Regulation 17 requires that a longitudinal deceleration of not less than 20 g is applied for 30 milliseconds in the forward direction of the vehicle[25]. The goal of this paper is to develop a quasi-static equivalent to this test, similar in approach to the static test in ISO 16840 [12] for wheelchair seating systems.

Since our review of the literature indicated no clear data for seat-base loading due to occupant and seat inertia during a frontal impact, two modelling approaches were adopted: an analytical free-body diagram-based approach and a multibody modelling approach implemented in MADYMO [23, 24]. The goal of the modelling was to establish the equivalent peak horizontal and vertical static seat-base loads and the peak bending moment during a standardized 20g frontal impact. These loads were then statically modelled on the proposed swivel base designs in a standard INSTRON uniaxial testing machine by means of custom designed jigs. These approaches are now described in more detail.

Analytical and multibody analysis to predict force and torque peaks

Analysis of standard seat using free-body diagram approach

The analytical model of the loading transmitted to the seat-base during a standardized frontal impact is obtained by applying D'Alembert's principle to the passenger's body and to the seat during the pulse and assuming dynamic equilibrium conditions. The forces acting on the two bodies are sketched in the two free-body diagrams shown in Figure 2 and Figure 3.

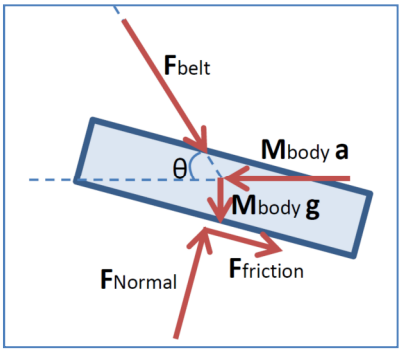

Figure 2 – Occupant free-body diagram.

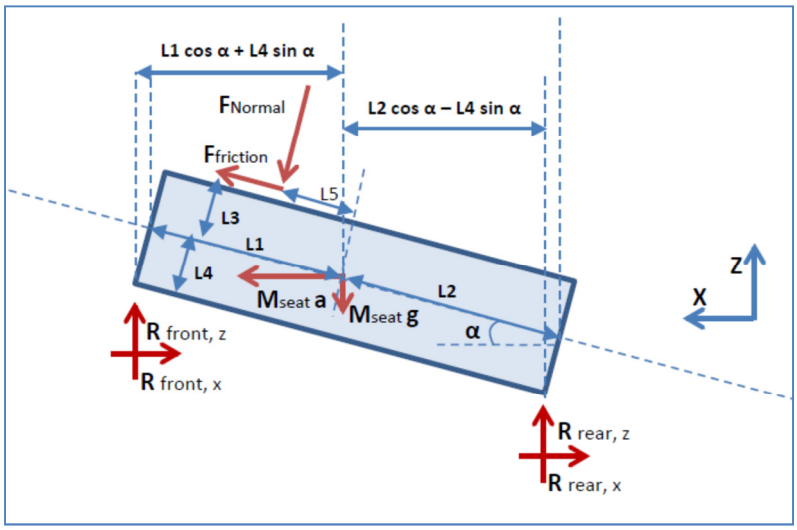

Figure 3 – Seat free-body diagram.

At each instant of the horizontal acceleration pulse (a), the human body is in dynamic horizontal and vertical equilibrium under the effect of the inertial force ($m_b a$), the gravity force ($m_b g$), the belt force F_{belt}, the friction force F_{fr} and the seat normal force F_N:

$$\sum F_{occupant,x} = m_b a - F_{belt}\cos\theta - F_{fr}\cos\alpha - F_N \sin\alpha = 0 \quad (1)$$

$$\sum F_{occupant,z} = -m_b g - F_{belt}\sin\theta + F_N \cos\alpha - F_{fr}\sin\alpha = 0 \quad (2)$$

The friction force F_{fr} is assumed proportional to the seat-passenger normal force through the Coulomb friction coefficient μ:

$$F_{fr} = \mu F_N. \quad (3)$$

The seat body is in equilibrium under the inertial force ($m_s a$), the seat-passenger friction and normal forces and the reaction forces R_{front} and R_{rear} of the seat base:

$$\sum F_{seat,x} = m_s a + F_{fr}\cos\alpha + F_N \sin\alpha - R_{front_x} - R_{rear_x} = 0 \quad (4)$$

$$\sum F_{seat,z} = -m_s g + F_{fr}\sin\alpha - F_N \cos\alpha + R_{front_z} - R_{rear_z} = 0 \quad (5)$$

$$\sum M_{seat,CG} = -R_{front_z}(L_1\cos\alpha + L_4\sin\alpha) - R_{front_x}(L_1\sin\alpha - L_4\cos\alpha) + R_{rear_z}(L_2\cos\alpha - L_4\sin\alpha) + R_{rear_x}(L_2\sin\alpha + L_4\cos\alpha) + F_N L_5 + F_{fr} L_4 = 0. \quad (6)$$

Finally the shear forces at the front and rear connection are assumed to be equal:

$$R_{front_x} = R_{rear_x}. \quad (7)$$

Therefore there are seven unknowns of the system ($F_{belt}, F_N, F_{fr}, R_{front_x}, R_{front_z}, R_{rear_x}$ & R_{rear_z}) and these can be found by solving the linear equations 1-7. The input parameters ($L_1, L_2, L_3, \alpha, L_4, L_5$) depend on the particular seat geometry under consideration.

Analysis of standard seat using multibody modelling approach

An equivalent multibody analysis has been carried out using the MADYMO software [23, 24]. The standard software library includes a frontal impact simulation with a 50%ile male Hybrid III dummy model (a_frontalel.xml), and this model was amended to represent the current loading scenario. A 20 g pulse in accordance with the lower corridor of UNECE Regulation 17 was set (Figure 4), the airbag system was removed and the appropriate virtual load cells were inserted to extract seat attachment constraint forces and moments. The seat, composed of a seat plane and cylinder and a seat back connected through a rotational spring, was rigidly fixed to the vehicle.

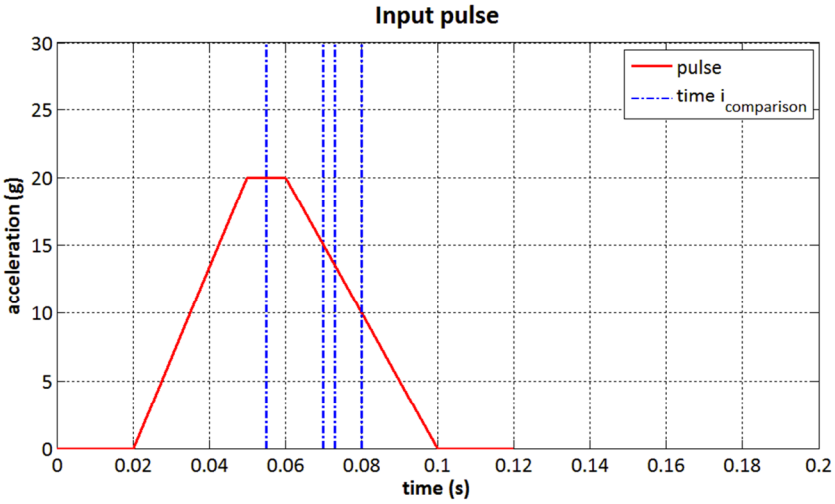

Figure 4 – Longitudinal acceleration pulse.

The three point belt system is composed of a finite element (FE) coupled with a multibody system (MB). The main components are the belts (FE), the retractor (MB), pretensioner (MB), height adjuster (MB), buckle (MB) and anchor points (MB), see Figure 5. The retractor is coupled with a load limiter device and the various belt parts are connected through rotational and translational springs. A friction function is defined between belt surfaces and dummy clothes.

The seat parts (planes and cylinder) are rigidly connected together and the position of the joint connecting the seat to the vehicle frame has been set at the location of the swivel bearing, see Figure 6.

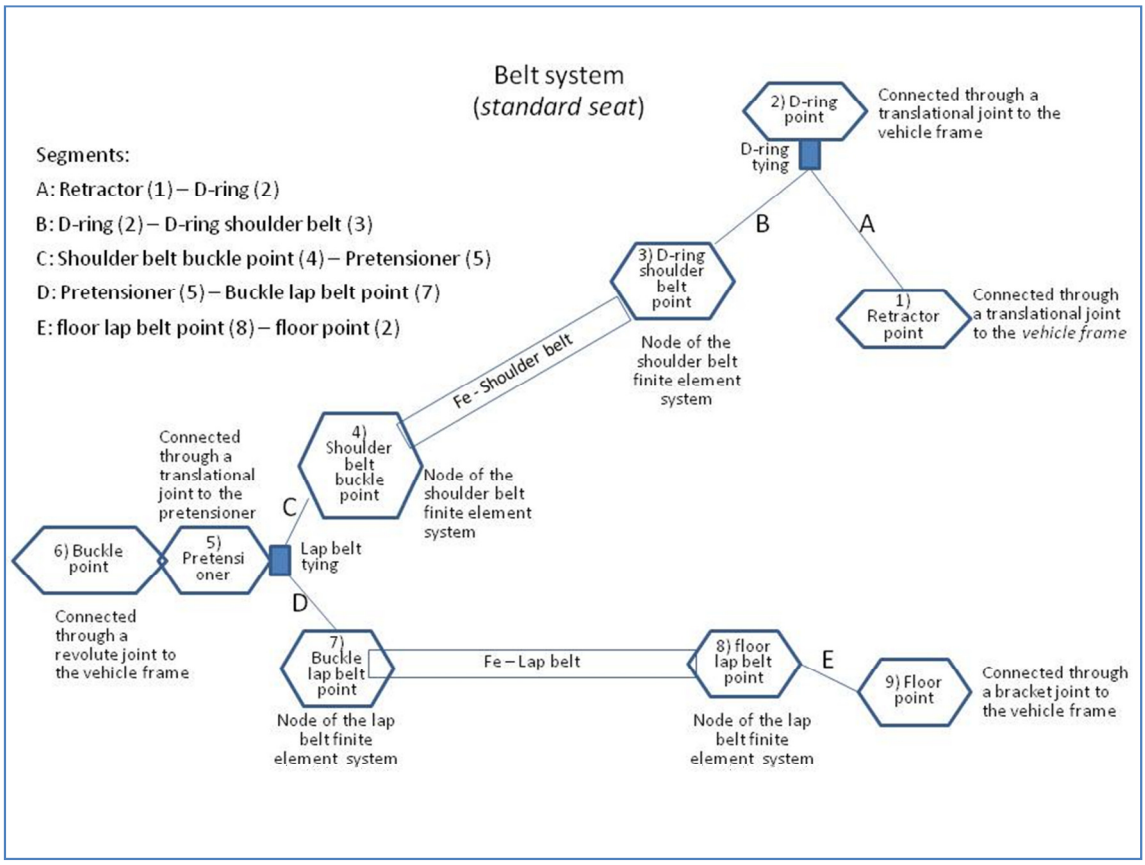

Figure 5 – Scheme of the MADYMO belt system for the standard seat.

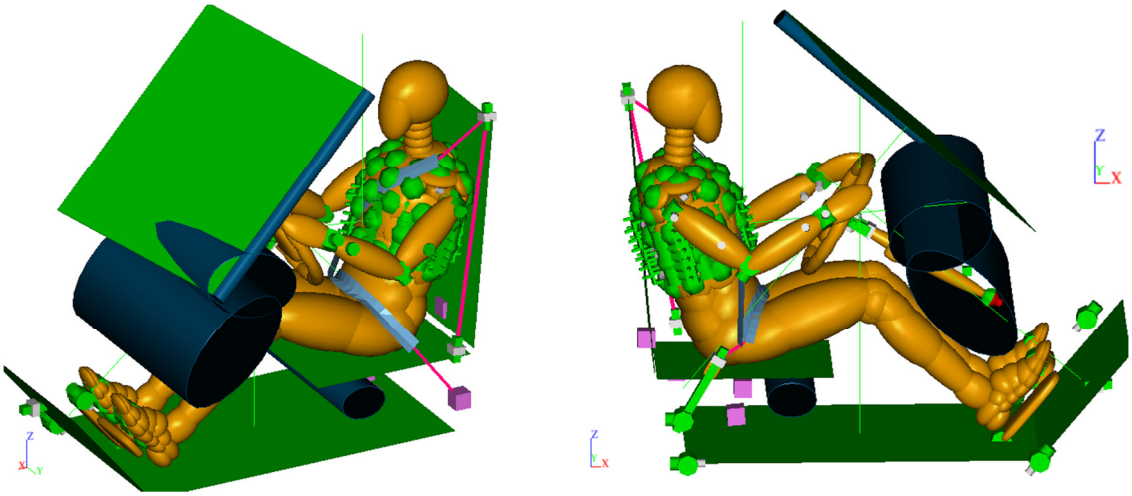

Figure 6 – MADYMO multibody model of a vehicle interior, seat and vehicle occupant.

Analysis of seat with integrated seatbelts using free-body diagram approach

In the case of the seat with integrated seatbelts the equilibrium equations of the seat need to take into account the additional belt force. Equations 4-5 become thus:

$$\sum F_{seat,x} = 0: \; m_s a + F_{belt}\cos\theta + F_{fr}\cos\alpha + F_N \sin\alpha - R_{front_x} - R_{rear_x} = 0 \quad (8)$$

$$\sum F_{seat,z} = 0: \; -m_s g + F_{belt}\sin\theta + F_{fr}\sin\alpha - F_N \cos\alpha + R_{front_z} - R_{rear_z} = 0 \quad (9)$$

However, because of the complexity of the model, the belt force has been assumed to have a null lever arm with respect to the pivot. Equation 6 has not been modified. Accordingly only the total horizontal and vertical seat base forces are accounted for in this approach.

Analysis of seat with integrated seatbelts using multibody modelling approach

In MADYMO the geometry of the seat model with integrated belts was based on the new Ford BMax seat. The main modification with respect to the standard model is given by connecting the belt retractor, height adjuster and anchor point directly to the seat.

For both MADYMO models (standard and with integrated seat-belt), pre-simulations were first used to find the occupants vertical equilibrium position under gravity and then the crash pulse (see Figure 4) was applied. The first part of the simulation lasts 1.0 s, this time being necessary to the dummy to make contact to the seat and to dissipate the inertial forces in the vertical direction.

Experimental testing of the swivel bases using a uniaxial testing machine

The static experimental testing of the swivel bases was carried out by applying the horizontal and vertical loads and the bending moment established from the MB and free-body diagram analyses previously described. These loads are intended to act as a static equivalent to the dynamic tests outlined in UNECE Regulation 17. To develop a testing procedure that could be easily reproduced, the tests were set up to be carried out with a uniaxial test machine.

Swivel base for standard seat

For the standard swivel base the loading was based on the reaction forces (Rx and Rz) calculated using the free-body diagram approach and validated through the MB model. Using these known horizontal and vertical loads and bending moment, the resultant load magnitude $F = \sqrt{R_x^2 + R_y^2}$ and direction $\beta = \tan^{-1}\frac{R_z}{R_x}$ were calculated. To simultaneously apply the normal and shear loads corresponding to the reactions (Rx and Rz) of the seat base under the prescribed pulse acceleration, two wedge shaped frames (jig) to hold the seat at an angle were designed, see Figure 7. One jig was bolted into the base plate of the uniaxial test machine and the swivel was connected to it while the second one was positioned on the seat, see Figure 8.

An INSTRON 5589 Electromechanical Universal Testing Machine was used to apply the static load. The loading was applied incrementally to the swivel seat base until the required test load was reached. After the prescribed load peak was reached the loading was increased up to the base critical maximum which was evaluated on inspection at each test.

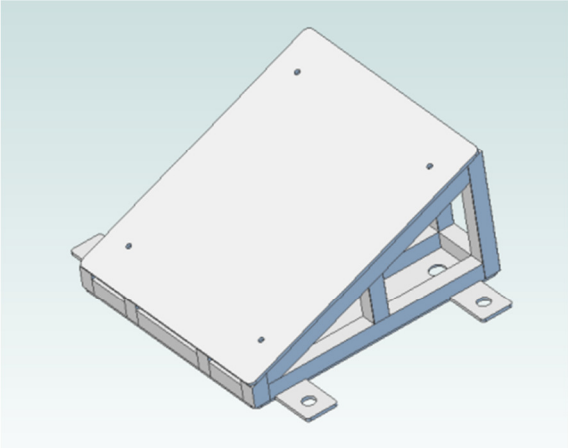

Figure 7 – Schematic of angled test jig

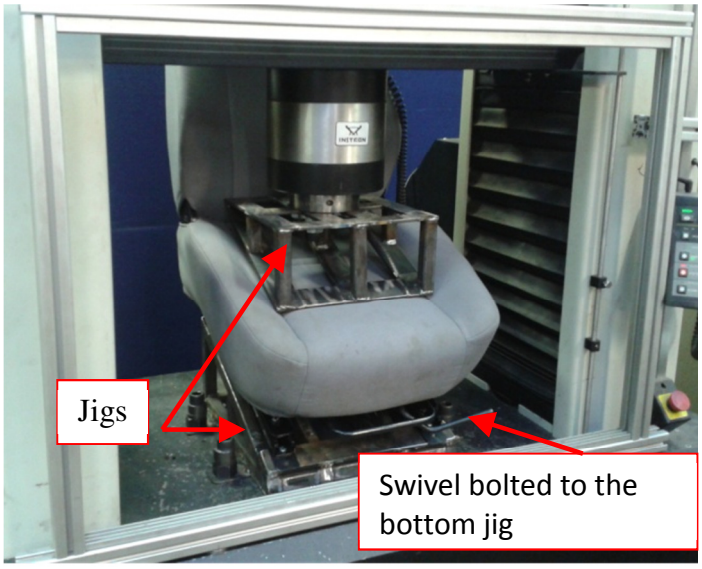

Figure 8 - Angled test jig in INSTRON 5589

Swivel base for seat with integrated seatbelts

Due to the complexity of the analysis of the seat with integrated seatbelt the MB model was used to obtain the peak loads on the swivel base rather than the analytical free body diagram (FBD) approach.

Since the maximum horizontal and vertical seat base reactions occur at different times, two different angled frames were designed to hold the swivel base at the required angle to represent the loading at these distinct times. Moreover to reproduce the torque acting on the seat base due to the upper seat belt mount an additional frame was fitted to the top of the swivel base. This approach allows the load to be applied at the correct distance from the centre of the swivel base. Figure 9 and Figure 10show the test rig and the layout and calculation scheme.

As for the standard base test, the load was applied incrementally until the calculated peak loads were reached. The loads corresponding to the maximum horizontal and vertical seat base reactions were applied to the same swivel base to ensure that it could

withstand both loading. The test was considered successful if the swivel seat mechanism remained locked for the calculated peak loads.

Figure 9 – Schematic of angled test jig

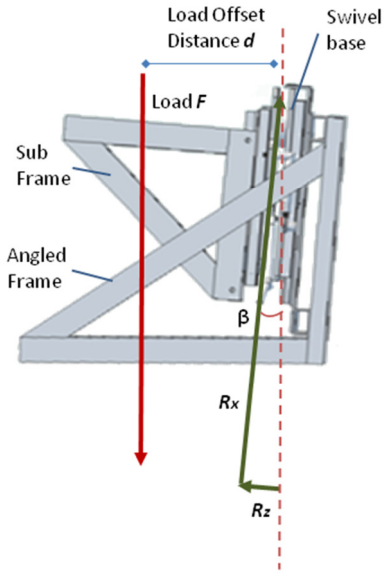

Figure 10 - Angled test jig in INSTRON 5589

Results

Analytical and multibody results

Standard seat

The free-body analysis was applied to the standard seat using the dimensions reported in Table 1. The same geometry was used for the MADYMO model. The analytical analysis was carried out for a longitudinal acceleration equal to 20 g while the numerical simulation was run using the acceleration pulse reported in Figure 4.

During the MB simulation the belt force angle varies from the initial value of 42° to a maximum of 57°. The initial belt angle value 42° was used for the free-body diagram approach.

Table 1 – Standard seat analyses: input values.

STANDARD SEAT ANALYSIS INPUT		ANALYTICAL MODEL		MADYMO MODEL	
seat dimensions	$L_1; L_2$	0.20	m	/	
	$L_3; L_4$	0.08	m	/	
	L_5	0.10	m	/	
	L_6	0.013	m	/	
	L_7	0.145	m	/	
seat angle	α	17	°	17	°
belt angle	θ	42	°	42-57	°
seat-passenger friction coefficient	μ	0.4		0.4	
dummy mass	m_b	80	kg	80	kg
seat mass	m_s	7	kg	7	kg
horizontal acceleration	a	20	g	0-20	g
inertial force	$(m_b + m_s)a$	17069	N		/
gravity force	$m_b g$	853	N	853	N

In Table 2 the numerical and the analytical results are reported. The force values obtained at time t=0.075 s, that is when the seat-base loading reaches the maximum value (Figure 11), are reported for the MB model.

Table 2 - Standard seat analyses: result comparison

STANDARD SEAT ANALYSIS RESULTS		ANALYTICAL MODEL		MADYMO MODEL		RELATIVE DIFFERENCES WITH RESPECT TO THE ANALYTICAL MODEL
belt force	F_{belt}	11759	N	10627	N	-10%
friction force	F_{fr}	4124	N	/		
seat normal force	F_N	10309	N	9781	N	-5%
seat-base reaction forces	R_{front_x}	4166	N			
	R_{front_z}	9051	N			
	R_{back_x}	4166	N			
	R_{back_z}	-330	N			
	R_x	8331	N	9784	N	17%
	R_z	8722	N	9848	N	13%

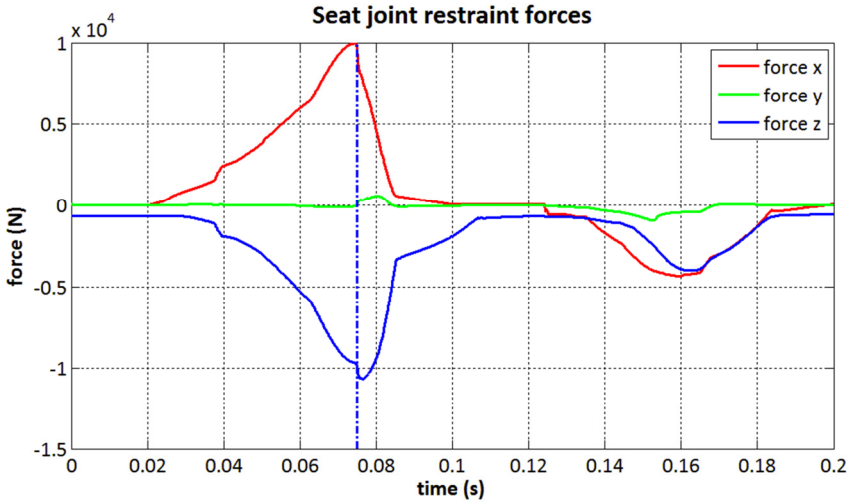

Figure 11 – Picture showing angled bottom and top jig in INSTRON Machine.

The comparison between the maximum belt forces (Table 2) shows that the two models are in good agreement with a maximum relative difference of 17%. The main difference between the two approaches is given by the acceleration of the occupant's body during the pulse. In the analytical approach the occupant is modelled as a rigid body having the same acceleration as the seat and the vehicle. In the MB simulation the occupant is simulated by the Hybrid III crash test dummy, whose body parts can accelerate relative to each other. Moreover the belt forces are limited by a load limiting retractor and they restrain only the thorax and the pelvis of the dummy. Also, the belt forces are delayed with respect to the vehicle inertial force since they are triggered 0.015 s after the pulse starts. No comparison is made between the friction forces in the two analyses because of the presence of the seat cylinder in the multibody model changes the ratio between the seat normal and shear forces.

Seat with integrated seatbelts

In the following graphs the results of the multibody simulation of the seat with integrated seatbelts are reported. In Figure 12 the forces transmitted by the belts to the

seat are plotted. The direction of the resultant belt force in the time interval chosen for the comparison with the analytical model is between 12° and 17° with respect to the horizontal. In Figure 13 and Figure 14 the seat bracket joint forces and torque are plotted. To gain a deeper understanding of the results achieved through the two analyses a comparison has been made in this case for different time and local peak pulse values (t=0.055 s, t=0.070 s, t=0.073 s and t=0.080 s). These times are indicated in the graphs by vertical dotted lines referred as time icomparison. At each time the belt force angle in the free-body analysis has been set equal to the value obtained by the multibody model and the horizontal input acceleration has been set according to the value of the pulse at that time. The results are reported in Table 3. The comparison between the two models is made in terms of the total seat joint forces, total belt force and normal seat force. In Table 3, a force balance for the occupant and seat body is also given.

Table 3 – Mounted-belt seat analysis: result comparison.

Analytical vs multibody results: A = analytical; MB = multibody.										
seat angle	α	0		0		0		0		deg
seat dimensions	$L_1 = L_2 = 0.25$; $L_3 = L_4 = 0.08$; $L_5 = -0.1$									m
analysis type		MB	A	MB	A	MB	A	MB	A	
Time	$i_{comparison}$	0.055		0.070		0.073		0.080		s
pulse acceleration value	a	20.0		14.5		13.0		9.5		g
pulse force value	$a(m_b+m_s)$	17.1		12.4		11.1		8.1		kN
belt force angle	θ	15.7		11.5		12.7		4.8		deg
belt force in x	$F_{belt,x}$	7.5	14.3	13.5	10.5	13.3	9.3	11.3	7.0	kN
belt force in z	$F_{belt,z}$	2.1	4.0	2.8	2.1	3.0	2.1	0.9	0.6	kN
seat force on the occupant body in x	$F_{seat,x}$	1.7	1.4	3.8	0.9	4.5	0.9	1.4	0.4	kN
seat force on the occupant body in z	$F_{seat,z}$	3.3	4.8	6.8	2.9	8.2	2.9	10.4	1.4	kN
seat base front force in x	$R_{front,x}$	/	8.5	/	6.2	/	5.5	/	4.1	kN
seat base front force in z	$R_{front,z}$	/	2.4	/	2.0	/	1.8	/	1.5	kN
seat base rear force in x	$R_{back,x}$	/	8.5	/	6.2	/	5.5	/	4.1	kN
seat base rear force in z	$R_{back,z}$	/	-1.6	/	-1.1	/	-0.9	/	-0.7	kN
seat joint force in x	R_x	10.3	17.1	17.9	12.4	18.3	11.1	13.0	8.1	kN
seat joint force in z	R_z	1.2	0.9	0.2	0.9	1.3	0.9	5.5	0.9	kN
seat joint torque in y	T_y	3.3	/	3.9	/	4.3	/	4.9	/	kN m
equilibrium of the occupant body in x:										
belt force	$F_{belt,x}$	7.5	14.3	13.5	10.5	13.3	9.3	11.3	7.0	kN
sum of other forces	$m_b\,a - F_{seat,x}$	14.0	14.3	7.6	10.5	5.7	9.3	6.1	7.0	kN
occupant body acceleration	a_b	-8.3	0	7.5	0.0	9.7	0.0	6.7	0.0	g
equilibrium of the seat body in x and z:										
forces balancing the seat base force in x	$F_{seat,x} + m_s\,a + F_{belt,x}$	10.5	17.1	18.3	12.4	18.7	11.1	13.4	8.1	kN
forces balancing the seat base force in z	$F_{seat,z} + m_s\,g - F_{belt,z}$	1.2	0.9	4.1	0.9	5.3	0.9	9.5	0.9	kN

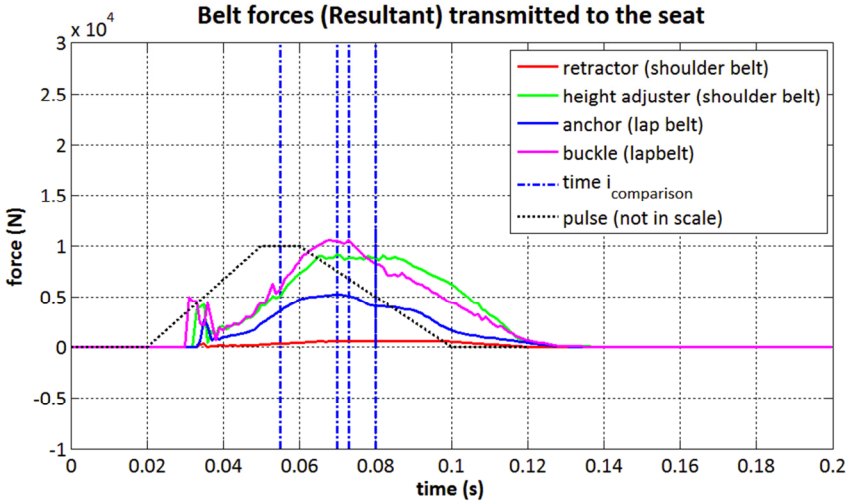

Figure 12 – Belt forces time histories (seat with integrated seatbelts).

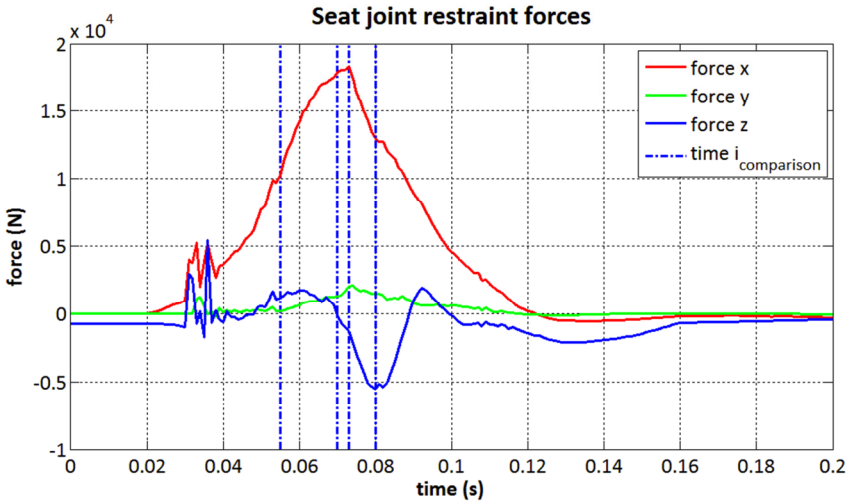

Figure 13 - Reaction forces acting on the seat base (seat with integrated seatbelts).

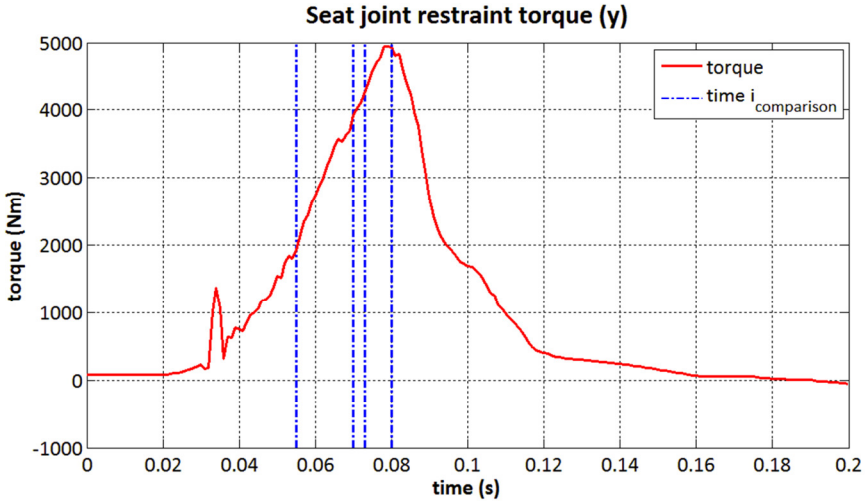

Figure 14 - Torque in the x-z plan acting on the seat base (seat with integrated seatbelts).

In the MB simulations the maximum horizontal joint force value is reached at t=0.073 s (Rx= 18.3 kN, Rz=1.3 kN, Ty=4.3 kNm) when the pulse has already decreased to 13 g

while the maximum torque and vertical seat joint force are reached at t=0.080 s for a pulse value of 9.5 g (Rx= 13.0 kN, Rz=5.5 kN, Ty=4.9 kNm). The free-body diagram analysis shows that the maximum horizontal joint force value is reached for the maximum acceleration value (20 g).

The comparison between the forces for each pulse value shows once again the effect of the complex MB/FE belt system which cannot be captured by the single body free-body analysis. Also, from the occupant body force balance it can be seen that the sum of the forces acting on it is not zero in the case of the MB simulation, and so the body is accelerated forward and backward during the pulse (with respect to the vehicle). The same result is shown by the plot in Figure 15.

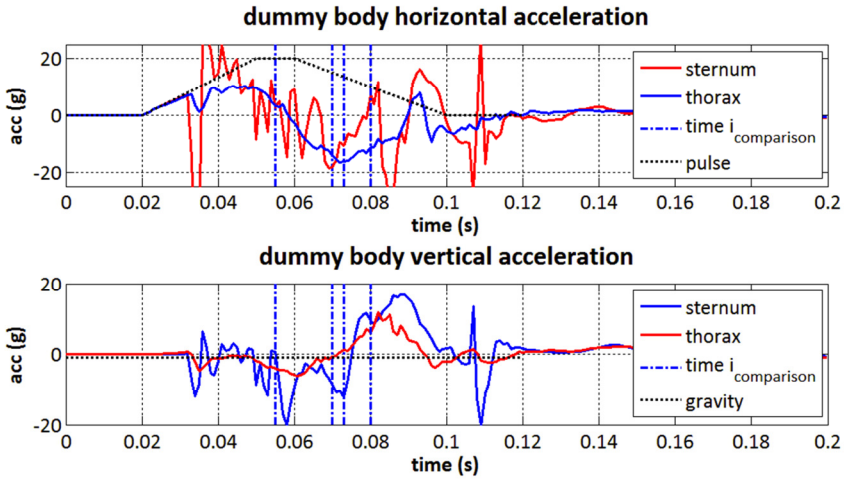

Figure 15 - Dummy sternum and thorax acceleration during the pulse.

In relation to the seat balance in the multibody model it must be noted that the seat joint forces and the sum of all the other forces acting on it are not exactly the same because of the presence of the spring connecting the belts to the seat. For sake of simplicity the forces relative to these restraints have not been included in the balance.

In spite of the difference between the results compared per each pulse value the two models give overall similar results: The maximum horizontal seat joint force for the MB model is in fact 18.3 kN while the one obtained through the free-body approach is 17.1 kN. As for the vertical seat joint force, since the seat angle is zero the vertical seat joint force of the analytical model does not depend on the horizontal acceleration and is equal to the total weight of the seat and occupant (0.9 kN). On the other hand the MB simulation shows the vertical and horizontal oscillation of the occupant's body under the horizontal pulse as well as the differential acceleration of the various body parts.

In conclusion the MB model better represents the complexity of the loading on the seat with integrated seatbelts and for this reason has been used to derive peak load levels for quasi-static testing of the swivel seat for the seat with integrated seatbelts.

Multibody model validation

In order to assess the reliability of the multibody model, published data for similar pulses were used [13]. In particular, of the four car seat tests reported in [13] , the car seat test A was simulated for its close resemblance with the original MB model

described previously. The test was carried out using a test-rig subjected to a 20 g acceleration; in order to evaluate the interaction between the seat and the passenger a 50-percentile hybrid III dummy was used. The dummy was secured to the seat by a three point belt system directly connected to the floor. Forces and/or accelerations were measured on the seat frame, the floor connections, the seat belt, the submarine-beam and on several locations in the dummy.

To simulate the experimental test the MB model previously described was modifies by replacing the bracket joint between the seat and the vehicle with four point restraints in the position of the load cells. The stiffness of the point restraints was selected to obtain a displacement of the point restraint of less that 1mm during impact (ie completely rigid joint). The seat geometry and angle was not changed but the submarine beam position was adjusted in order to fit the real test geometry. The same pulse function applied in the test was used for the simulation.

In Figure 16 the experimental seat-floor connection forces have been plotted and compared to the MB ones. The comparison clearly shows similar experimental and numerical peak values; maximum relative differences of 3% and 10% along the longitudinal and vertical directions respectively are calculated.

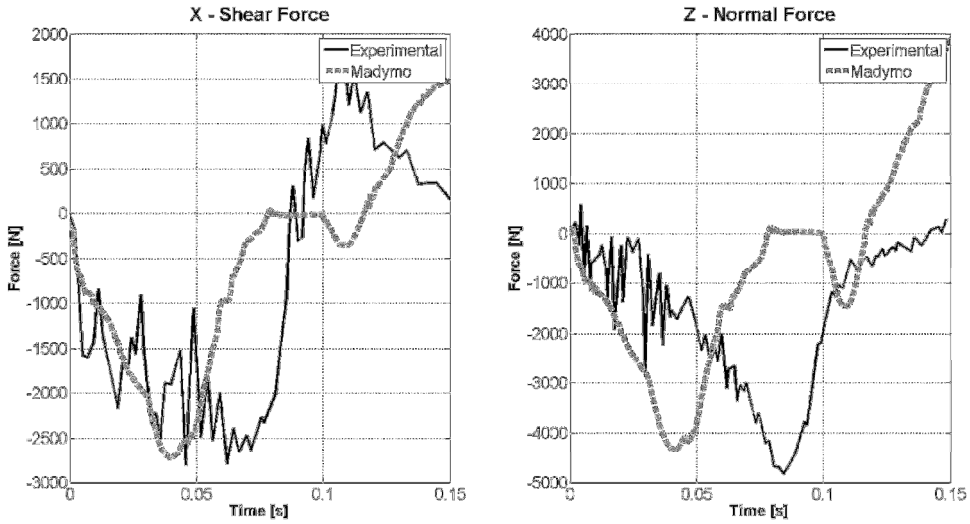

Figure 16. Comparison of seat joint connection forces: experimental [13] vs multibody.

Experimental results

Swivel base for standard seat

The load values for the static test on the swivel base, based on free body analysis results (Table 2) are reported in Table 4.

Table 4 – Components and resultant of the load applied to the swivel base for standard seat.

SEAT BASE LOAD		
Horizontal Reaction	R_x	8.7 kN
Vertical Reaction	R_z	8.3 kN
Resultant Load	R	12.0 kN

The calculated load was applied in increments of 3 kN up to a maximum of 12 kN. A preload of 0.1 kN was applied to the system to remove slack. The deflection was measured between the two base plates of the swivel base at marked points on each corner. A maximum downward deflection of 9 mm was measured at the front left measurement point. After the calculated peak load was reached the load was increased up to 24 kN for observation purposes. The test was then interrupted for safety reasons although the swivel base was still fully functional.

Swivel base for seat with integrated seatbelts

The procedure for testing the Swivel base for the seat with integrated seatbelt was similar to that used for the standard seat base. The applied loads derived from the MB results (see Table 3) are reported in Table 5.

Table 5 - Load patterns for the swivel base for seat with integrated seatbelts.

PEAK HORIZONTAL LOAD PATTERN				PEAK VERTICAL LOAD PATTERN		
Torque	T	4.3 kNm		Torque	T	4.9 kNm
Load	F	18.3 kN		Load	F	14.1 kN
Horizontal reaction	R_x	18.3 kN		Horizontal reaction	R_x	13.0 kN
Vertical reaction	R_z	1.3 kN		Vertical reaction	R_z	5.5 kN
Resultant angle	β	4°		Resultant angle	β	23°
Load offset distance	d	0.23 m		Load offset distance	d	0.35 m

After the rig was preloaded to 0.1KN to remove slack, the peak horizontal load pattern was applied. The swivel base was then transferred to the frame designed for the vertical peak load, the preload was applied again and the swivel design was tested by increasing the force up to the calculated vertical load. Finally the swivel base was attached again to the first angled frame and tested until visible deformation was observed, see Table 6. The test was interrupted after a load of 28 kN was reached. At this stage the sliding rails had begun to collapse but overall integrity was maintained.

The test was evaluated visually (see Table 6). The base had minimal permanent deformation during the first two loading cycles and the test was considered successful. The swivel base was still operational after the critical load was reached although it was not able to rotate fully as the sliding rails had begun to collapse during the final loading.

Table 6 – Test results for the swivel base for seat with integrated seatbelts.

TEST	TORQUE	LOAD	RESULT
Peak horizontal load pattern - MB Calculated load	4.3 kNm	18.3 kN	Pass
Peak vertical load pattern - MB Calculated load	4.9 kNm	14.1 kN	Pass
Peak horizontal load pattern - Maximum Capacity	6.5 kNm	28.0 kN	Pass

Discussion

Our review of the literature showed no guidance for the frontal impact evaluation of swivel seat crashworthiness. Accordingly, in this paper a proposed quasi-static test method is presented for application prior to dynamic sled testing. The main advantages of the proposed quasi-static test method for testing the crashworthiness of swivel seat products are cost efficiency and ease of application. The quasi-static test is intended to load the seat base with the forces that would act on it if a 20 g frontal impact pulse was applied to the seat and vehicle occupant. These forces are obtained using two different approaches, a free-body analysis and multibody modelling.

The method has been applied both to a standard seat and to a seat with integrated seatbelts and the comparison between the two analysis methods shows horizontal seat joint forces which differ by less than 20% for both seat types. Both methods have advantages and drawbacks. The free-body approach is particularly simple to use and can give a good estimation of the horizontal forces acting on the seat base during the pulse. In the case of the standard seat the comparison with the MB model has also shown that the estimation of the vertical force acting on the seat base is similar (13% difference). On the other hand the free body method does not take into account the dynamical response of the occupant's body and can overestimate the loading on the seat base depending on the seatbelt maximum force set by the load limiter device. Another uncertainty of the FBD model is the angle of the total seatbelt force during the pulse.

The multibody analysis obviously gives a deeper understanding of the phenomenon and has been presented here with this purpose. Moreover the MB model shows the effect of the differential motion of the occupant's body parts on the whole seat response. For example, the vertical force acting on the seat base as a consequence of the horizontal pulse was not predicted by the free-body approach in the case of the seat with integrated seatbelt, see Table 3. Since the seat angle was zero for this case the force is clearly due to the oscillation of the occupant's body under the restraint of the various seatbelt components.

The multibody modelling for the standard seat has been validated using experimental data obtained from a similar seat tested using a test-rig and a 20 g acceleration pulse. The validation has shown that the vertical position of the submarine beam can affect the maximum load values acting on the seat connections and thus on the swivel adaptation. This vertical position is quite high in the proposed MB model and thus the simulation is likely to provide load predictions which err on the safe side.

Moreover the comparison with experimental seat testing has shown that it is reasonable

to assume a rigid connection between seat and vehicle. Also in this case the assumption will provide safe loading values for the swivel adaptation.

In the view of providing an easy-to-use tool for enterprises who want to test swivel seat adaptations the MB modelling approach is disadvantaged by the necessity of mastering a MB software and by the cost of the software license. However, in our future work we intend to perform a parametric analysis on the effects of the seat geometry on the forces and torques experienced by the swivel base in a frontal impact. This analysis will clarify for which cases the free-body approach is not sufficiently refined.

With regard to the experimental testing of the two swivel bases, the paper has shown two possible different ways of carrying out the test using a uniaxial loading machine. In the first case (standard seat) the swivel base was attached to the original seat and the load was applied using two angled steel jigs (Figure 9 and Figure 10); in the second case the seat was simulated using two different steel frames through which both the resultant force and torque were applied (Figure 11). The economic and logistic advantages of both using a uniaxial machine and testing only the swivel base or the swivel base attached to the seat are obvious if compared to carrying out a sled test.

Nonetheless, this approach is not intended to replace the UNECE Regulation 17 test, but rather to give designers a preliminary test for evaluating new prototypes prior to dynamic sled testing a final design. This approach is similar to the static seat testing Annex of ISO 16840 [12] for assessing the crashworthiness of wheelchair seating systems.

Conclusion

This paper outlines a process to ensure that swivel seat adaptations meet a self enforced standard that is in line with the UNECE Regulations. The process was also designed to aid the development and design of new swivel seat base products, to highlight weak areas of the design and facilitate improvements throughout the prototype stages.

The paper presents a quasi-static test to perform on swivel seat adaptation and two possible approaches for calculating the loads to apply: a simple and easy to use free-body diagram approach and a more detailed multibody modelling approach. The analyses have been carried out on a standard seat and on a seat with integrated seatbelts. The comparison of the results has indicated that both methods are reliable for standard seats although future work will clarify the range of use of the simple analytical approach depending on the seat geometry in the case of the seat with integrated seatbelts. An experimental validation of the MB approach has also been undertaken using experimental published data.

To the authors knowledge this is the first approach of this kind for the assessment of swivel seat frontal impact crashworthiness.

Appendix A: Swivel test procedure for standard seat

The testing procedure of a swivel seat adaptation can be resumed in two main steps:

- calculating the static peak loads (R_x , R_z, and T_y) and corresponding resultant load having magnitude $F = \sqrt{R_x^2 + R_y^2}$ and direction $\beta = \tan^{-1}\frac{R_z}{R_x}$.
- applying the static loading incrementally up to the peak value to a swivel joint attached to the vehicle seat.

For standard seat the static peak loads can be calculated solving the linear equation system reported in section "Analysis of standard seat using free-body diagram approach" or running a multibody simulation using the pulse acceleration function reported in Figure 4, see section "Analysis of standard seat using multibody modelling approach".

For seat with integrated seatbelts the static peak loads should be calculated running a multibody simulation using the pulse acceleration function reported in Figure 4, see section "Analysis of seat with integrated seatbelts using multibody modelling approach".

The test can be carried out both by testing the swivel joint alone or the swivel joint attached to the seat. In both cases steel frames will need to be designed in such a way to apply the machine vertical load $F = \sqrt{R_x^2 + R_y^2}$ with an angle $\beta = \tan^{-1}\frac{R_z}{R_x}$ to the swivel/seat. To take into account the calculated torque Ty the resultant F will be applied at a distance d = Ty / F from the CG of the seat.

Since maximum shear and normal forces will not occur necessarily at the same time, two different loading patterns can be applied: one for maximum shear force and one for maximum normal force.

The test will be considered passed if the swivel seat does not undergo major deformation and is still functional when unloaded.

References

[1] D. Adomeit, *Seat design—a significant factor for safety belt effectiveness* in *Twenty-Third Stapp Car Crash Conference Paper*, SAE, 1979.

[2] N. Bourdet, and R. Willinger, *Modeling of car seat and human body interaction under rear impact*, International Journal of Crashworthiness 11 (2006), pp. 553-560.

[3] L. Cabrolier, R. D'Souza, G. Bertocci, J. Tiernan, and C. Simms, *The Influence of Shoulder and Pelvic Belt Floor Anchorage Location on Wheelchair Occupant Injury Risk: a simulation study*.

[4] E. Esfahani, D. Marzougui, K. Digges, and C. Kan, *Effect of increase in weight and stiffness of vehicles on the safety of rear seat occupants*, International Journal of Crashworthiness 16 (2011), pp. 309-318.

[5] A. Gavelin, M. Lindquist, H. Haggblad, and M. Oldenburg, *Methodology for mass minimisation of a seat structure with integrated safety belts constrained by biomechanical responses on the occupant in frontal crashes*, International Journal of Crashworthiness 15 (2010), pp. 343-355.

[6] A. Gavelin, M. Lindquist, and M. Oldenburg, *Modelling and simulation of seat-integrated safety belts including studies of pelvis and torso responses in frontal crashes*, International Journal of Crashworthiness 12 (2007), pp. 367-379.

[7] ---, *Numerical studies concerning upper neck and head responses in frontal crashes with seat-integrated safety belts*, International Journal of Crashworthiness 12 (2007), pp. 465-479.

[8] R. Ge, Z. Lu, and F. Zhao, *Research of front seat design parameters on rear seat passenger safety*, IEEE, pp. 520-523.

[9] W. Golinski, and C. Gentle, *Biomechanical simulation of whiplash - some implications for seat design*, International Journal of Crashworthiness 6 (2001), pp. 573-583.

[10] A. Hault-Dubrulle, F. Robache, P. Drazetic, H. Morvan, C. Landsheere, and O. Luc, *Analysis of train driver protection in rail collisions: Part II. Design of a desk with improved crashworthiness performance*, International Journal of Crashworthiness 18 (2013), pp. 194-205.

[11] J. Hu, J. Wu, M.P. Reed, K.D. Klinich, and L. Cao, *Rear seat restraint system optimization for older children in frontal crashes*, Traffic injury prevention 14 (2013), pp. 614-622.

[12] ISO, ISO 16840-4 seating systems for use in motor vehicles, International Organisation for Standardisation, 2008.

[13] P. Lovsund, G. Nilson, T. L, Y. Haland, and S.E. Svensson, *A test rig for parametric studies of the car seat*, in *SAE paper no 93047*, 1993.

[14] M. Luo, and Q. Zhou, *A vehicle seat design concept for reducing whiplash injury risk in low-speed rear impact*, International Journal of Crashworthiness 15 (2010), pp. 293-311. Available at <Go to ISI>://000280281200006.

[15] R. Menon, Y. Ghati, and P. Jain, *MADYMO simulation study to optimize the seating angles and belt positioning of high back booster seats*.

[16] K. Mroz, O. Boström, B. Pipkorn, J. Wismans, and K. Brolin, *Comparison of Hybrid III and human body models in evaluating thoracic response for various seat belt and airbag loading conditions*.

[17] G. Nilson, *Effects of seat and seat belt design on car occupant response in frontal and rear impacts: a study combining mechanical and mathematical*

modelling, ed, Department of Injury Prevention, Chalmers University of Technology, 1994.
[18] D.P. Parent, J. Kerrigan, and J. Crandall, Comprehensive computational rollover sensitivity study part 2: Influence of vehicle, crash, and occupant parameters on head, neck, and thorax response, SAE Technical Paper, 2011.
[19] Y. Park, and G. Park, *Crash analyses and design of a belt integrated seat for occupant safety*, Proceedings of the Institution of Mechanical Engineers Part D-Journal of Automobile Engineering 215 (2001), pp. 875-889.
[20] H. Serber, *Test Results on the Counter Balanced Motion (CBM) SEAT Crashworthiness*, SAE SP (2003), pp. 17-24.
[21] S. Shaheen, and D. Niemeier, *Integrating vehicle design and human factors: Minimising elderly driving constraints*, Transportation Research Part C (2001), pp. 155-174.
[22] Y. Shi, I.T. Lee, A.M. Afsar, and J.I. Song, *Development and performance analysis of an automotive power seat for disabled persons*, International Journal of Automotive Technology 10 (2009), pp. 481-488. Available at http://dx.doi.org/10.1007/s12239-009-0055-8.
[23] TNO, *MADYMO Reference Manual,* 7.3 ed, TNO Automotive, 2010.
[24] ---, *MADYMO Theory Manual,* 7.3 ed, TNO Automotive, 2010.
[25] UNECE, Regulation 17 Uniform Provisions Concerning The Approval of Vehicles With Regard to the Seats, Their Anchorages and Any Head Restraints, 2002.
[26] US Department of Transportation, *Federal Motor Vehicle Safety Standards and Regulations*, in *Standard No. 208; Occupant crash protection.* , Federal Motor Carrier Safety Administration.
[27] L. Van Rooij, C. Sherwood, J. Crandall, K. Orzechowski, and M. Eichelberger, *The effects of vehicle seat belt parameters on the injury risk for children in booster seats*, SAE transactions 112 (2003), pp. 470-482.
[28] L. Wagstrom, A. Kling, H. Norin, and H. Fagerlind, *A methodology for improving structural robustness in frontal car-to-car crash scenarios*, International Journal of Crashworthiness 18 (2013), pp. 385-396.
[29] Y. Zhang, C. Ju, G. Yue, X. Chen, and H. Sun, *Simulation Analysis of the Rear Seat Female in Front Impact*, IEEE, pp. 767-770.